Characterization of drying behavior and modeling of industrial drying process

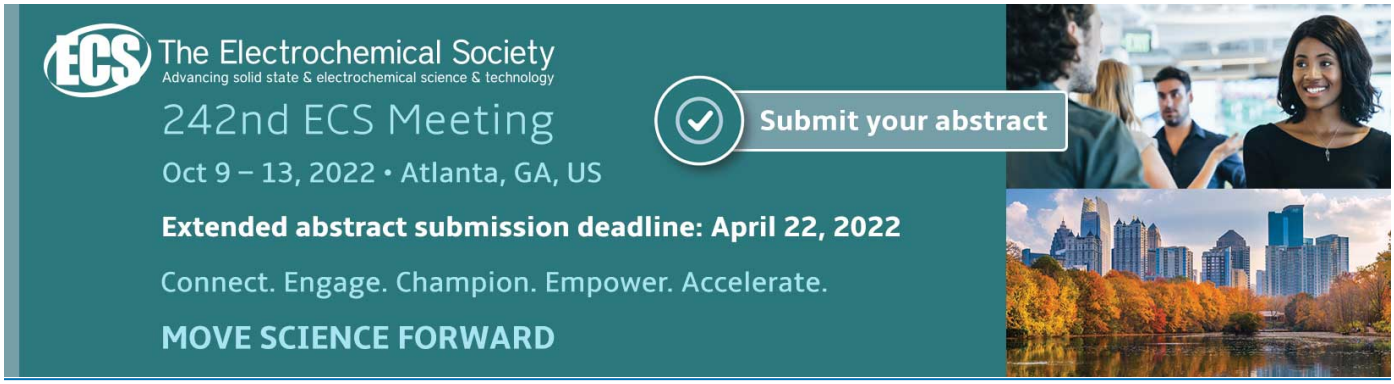

Characterization of drying behavior and modeling of industrial drying process

M Vasić and Z Radojević
"Institute for testing of materials", Bulevar vojvode Mišića 43 1100 Belgrade, Serbia

E-mail: milos.vasic@institutims.rs

Abstract. The general method for industrial chamber dryer optimization was reported in this paper. The first step in finding the most suitable drying regime is to characterized the clay raw material, especially its water loss at 2000C and to determine the critical drying rate inside the specially constructed laboratory dryer. These data provides us information if the product or the dryer is the bottleneck for the optimisation. If the optimization is justified geometry of the dryer, air mass flows, temperature, and humidity profiles inside the dryer as well as initial water content in the drying material, initial temperature of the products and the load of the dryer are required. Some of the previously mentioned data are only used to check if the chamber dryer is working properly, while the others are used as the initial parameters necessary for software simulation. In this paper two models for calculating the optimal drying parameters were used. The first model was developed from the comprehensive theory of the moisture migration during isothermal drying. The calculation software for setting up the non - isothermal drying regimes was reported in our previous papers. It is important to say that this model was not able to adequately predict the temperature raise within the drying products. In order to simulate the raise of the temperature of the roofing tiles during drying the second model was used. This simple receding drying front model was firstly reported by Kitcher. If both models are used simultaneously it is possible to calculate air temperatures, product temperature, absolute and relative humidity of the drying air, moisture content of the product, drying rate etc... It is important to mention that this approach can lead to the recommendations for changes inside the dryer before an optimized situation is achieved. One example of such situations is described in this paper in details.

1. Introduction

An experimental growth in drying requests and demands on a global scale has been registered during the last fifty years. It is expected that the closer interaction between the scientific community and industry will very soon find a way how to increase the quality of the dried products and to reduce the energy consumption. This will consequently lead to the optimization of the existing drying technologies and development of the new one. Future perspectives has to be directed towards material property determination, drying models validation, implementations of advanced coupling multi-physic modeling on the conjugate or semi-conjugate level. Computer-aid drying process engineering has become the generator of novel optimizing solutions and next-generation drying technologies. Even

though different approaching and modeling techniques as well as specialized user-friendlier software's were reported for describing the simultaneous heat and mass transport process during drying, an universal and widely applicable solution for optimization of the industrial dryers in the heavy clay industry is still not commercially available on the market. H. Shoukouhmand has developed the method for an accurate simulation of the air circulation devices, inlet air temperature and its humidity, flow rates, as well as drying process control parameters for a typical chamber dryer in the brick/ceramic industry. The set of partial differential equations governing heat and mass transport in a single brick domain together with the respective temperature and humidity boundary conditions were solved numerically in this study using finite element method [1]. Group of authors from Brazil has numerically studied drying of an industrial hollow brick in the laboratory chamber dryer at different temperatures. The drying and heating kinetic curves showed good agreement with the experimental data. The brick temperature and water mass fields showed an asymmetrical behavior, which is different from the studies in which only the brick domain was considered. The assumption of constant convective heat and mass transfer coefficients on all walls of the material was experimentally confirmed. It was also verified that these values were dependent on the brick position inside the dryer. It was registered that the air flow through the holes of the material was lower than the air flow around the brick, as a consequence of the brick position inside the kiln. That was the reason why the time for heating up and drying the inner brick walls was longer [2]. G. Dolanc has showed that properties of the outgoing drying air inside the chamber dryer can be directly controlled by adapting the air velocity. The applied system has successfully control the position of the inlet damper in a way that the humidity of the outgoing waste air remains constant without respect to the water content of the green ware. It was confirmed that when the air flow rate is decreased by circulating in a dryer for a longer period the air approaches closer to the cooling limit state. Thus the humidity of the waste outgoing air is raised and its temperature is decreased. According to the authors decreasing the flow rate results in a smaller amount of supplied energy per time unit, but the ratio between dissipation energy and supplied energy also becomes smaller. By measuring the humidity and flow rate of the waste air in the outlet channel it is possible to interactively adapts the damper in the inlet of the chamber [3]. E.Mancuhan has reported a solution how to avoid the risk of condensation during drying of brick in a tunnel dryer. Optimization was realized by finding the optimal values of the hot and outdoor air flow rates and stack temperatures at different outdoor temperatures and relative humidities. The optimum stack temperature and relative humidity were reported as 47°C and 80% respectively when the drying air is composed of the hot air at 200°C and outdoor air at 30°C with relative humidity of 40% [4]. Group of authors from Germany has reported the procedure for increasing the energy efficiency of dryers and simulation of the drying curve. The dependency of the moisture diffusion coefficient on the moisture fraction was firstly discussed [5]. On the base of such determined moisture diffusion coefficient the simulation of the drying curve and product shrinkage was possible. It is important to say that the model outputs were: time dependent moisture and shrinkage profiles, drying curve, evaporation rate as well as the calculated air temperature and product surface and/or core temperature change during drying [6,7]. Group of authors from Netherlands has outlined a procedure for optimization of the industrial chamber or tunnel dryers. This procedure requires drying of the full-sized products in a laboratory dryer, characterization of the industrial dryer, and computer-aid simulation of the drying process. The reported DrySim software uses the receding front drying theory for the mathematical description of the drying process. This software allows the user to build its own dryer with predefined components. If the local air temperature, air relative humidity and heat-transfer coefficient as a function of time are available the drying rate, product temperature and the position of the drying front can be simulated [8,9]. Vasic and the group of authors from Serbia have firstly presented a comprehensive theory of moisture migration during drying. Presented model for determination of the time dependent effective diffusivity was used for identification and tracking off all possible mechanisms of moisture transport and their transition from one to another during the constant and the falling drying period. It was stated that the capillary flow is predominant mechanism within the constant drying period, while in the falling drying period, the evaporation – condensation and vapor

diffusion were the predominant mechanisms [10]. This procedure was then applied for defining the theoretical optimal non isothermal drying regime in which the mass transport during drying was rigorously controlled. The drying process was divided into 5 segments. The duration of the first four drying segments was specified as the timescale period registered in different isothermal experiments, delimited with the help of the various characteristic points. Total drying time was reduced. The scarp rate inside the dryer was decreased. Dried roofing tiles had physico-mechanical properties higher than the limiting one specified within EN 1304 norm [11]. Vasic has recently compared and evaluated the Sebian model with the one reported by the German group of authors. Results have shown the absence of cracks on dried and fired samples. In the case of German method total drying time, as well as twist and camber coefficients were higher while the physico - mechanical properties were lower. These results have confirmed and additionally validated that the developed dying model can be used for the accurate prediction of industrial drying kinetics and a reliable estimation of moisture transport during drying [12].

2. Materials and Methods

The main goal of this paper was to report the general procedure which could be used for industrial dryer optimization. The first step was to record the actual industrial drying regime. The Serbian procedure for setting up the non-isothermal drying regime is than applied [11]. It is important to state that the raw material characterization is the integral part of the previously mentioned procedure. Calculated drying air (humidity, temperature and velocity) parameters were than compared with the one used in the industrial dryer. The next step was to o determine the critical drying rate inside the specially constructed laboratory dryer. These data provides us information if the product or the dryer is the bottleneck for the optimization. If the optimization is justified geometry of the dryer, air mass flows, temperature, and humidity profiles inside the dryer as well as initial water content in the drying material, initial temperature of the products and the load of the dryer are collected. Finally the second drying model was applied.

2.1 Mathematical description of the second drying model

When the critical point is reached (moment when the falling rate period starts) an evaporation front emerge and gradually moves into the interior of the body. During drying the position of the receding evaporation front is changing and the product is divided into two zones: the wet and dry one. In the dry zone, the free water content is zero and the main mechanism of moisture transfer is vapor flow. The set of equations which are used for description of the coupled heat and mass transport were defined for the dry zone, wet zone and at the receding boundary.

2.1.1 The wet zone

$$\frac{\partial X_{fw}}{\partial t} = \frac{\partial}{\partial z}\left(\delta_l \frac{\partial X_{fw}}{\partial z}\right);\quad c_{p,w}\frac{\partial T_1}{\partial t} = \frac{\partial}{\partial z}\left(\lambda_{eff}\frac{\partial T_1}{\partial z}\right); \tag{1}$$

Where $\delta_l, c_{p,w}, X_{fw}$ and λ_{eff} are respectively the liquid transfer coefficient, the specific heat capacity of water, the moisture content of free water and the effective thermal conductivity.

$$\lambda_{eff} = \lambda_l + \frac{\delta_v' \widetilde{M}_v}{RT}\frac{\partial P_v^*(T)}{\partial T}\Delta \mathrm{h_v};\ \delta_v' = \delta_v\left(1 + \frac{\frac{k_g K P_v}{\eta}}{\delta_v + \frac{k_g K}{m\eta}(P_g - P_v)}\right) \tag{2}$$

Where $\lambda_l, \Delta h_v, P_v^*(T), \delta_v', m, k_g, \eta$ and δ_v are respectively the thermal conductivity of liquid, the evaporation enthalpy, the saturation vapor pressure, the vapor transfer coefficient (which summarize the mutual effect of both convective and diffusive flows), the ratio of air and vapor diffusion

coefficient, the relative permeability of gas phase, the dynamic viscosity and the vapor diffusion coefficient.

2.1.2The dry or sorption zone

$$\rho \frac{\partial X_{sorb}}{\partial t} = \rho \frac{\partial}{\partial z}\left(\delta_{sorb} \frac{\partial X_{sorb}}{\partial z}\right) + \frac{\partial}{\partial z}\left(\frac{\delta_v' \widetilde{M_v}}{RT} \frac{\partial P_v}{\partial z}\right); \quad \rho c_{p,v} \frac{\partial T_2}{\partial t} = \frac{\partial}{\partial z}\left(\lambda_v \frac{\partial T_2}{\partial z}\right) \tag{3}$$

Where $c_{p,v}, \lambda_v, X_{sorb}$, and δ_{sorb} are respectively the specific heat capacity of vapor, thermal conductivity of vapor, the adsorbed water content and the adsorbed water transfer coefficient.

It is important to mention that for a non-hygroscopic material, X_{sorb} is zero and δ_{sorb} is negligible.

The mass and heat transfer at the receding boundary

2.1.3The receding boundary

$$\rho \delta_l \frac{\partial X_{fw}}{\partial z} = \rho \delta_{sorb} \frac{\partial X_{sorb}}{\partial z} + \left(\frac{\delta_v' \widetilde{M_v}}{RT} \frac{\partial P_v}{\partial z}\right); \lambda_{eff} \frac{\partial T_1}{\partial z} = \lambda_v \frac{\partial T_2}{\partial z} + \Delta \mathrm{h_v} \frac{\delta_v' \widetilde{M_v}}{RT} \frac{\partial P_v}{\partial z}; T_1 = T_2; X_{fw} = 0 \tag{4}$$

If the sorption isotherm, Bigoth drying curve (which is used for calculation of the actual drying surface during drying), local air temperature, air relative humidity and heat transfer coefficients as a function of the time are available it is possible to solve previously presented equation sets and to simulate the drying process, calculate the drying rate, product temperature and the actual drying front position.

The actual industrial drying regime was registered with TMI-Orion "CeriDry" data logger. This logger resolution was 0.04°C, 0.05% and 0.01 mm respectively for temperature, relative humidity and shrinkage. Registered drying regime is presented on figure 1. The next step was to characterize the raw material. Classical silicate analysis, XRD, particle size determination, and dilatometry test were carried on. These results were in detail reported in the reference [13]. The raw material was then milled until the whole content has passed through the sieve of 5 mm. Collected material was at the same time moisturized and grinded in the laboratory rotor crusher which gap was slowly reduced from 3 to 1 mm. Laboratory tiles (120 x 50 x 60 mm) were formed in the extruder "Hendle" type 4, under a vacuum of 0.8 bar. The next objective was to define the variable air parameters using the comprehensive drying theory. Drying air humidity was kept constant at 80, 70 and 60% respectively in each corresponding isothermal set. The drying air temperature in the first experiment of each series was set to 30°C. The drying air temperature was than raised for 5°C in each following experiment. In each experiment the drying air velocity was set to 3 m/s. The tile mass and the linear shrinkage were continually monitored and recorded. Measuring devices accuracies was 0.01 g and 0.2 mm. Drying air parameters were regulated inside the dryer. The accuracies of these measurements were ±0.2°C, ±0.2% and ±0.1% for temperature, humidity and velocity, respectively. These results along with the recommended drying regime were reported in the reference [11]. The next step was to determine the critical drying rate. The initial cooling limit temperature was 20°C. The starting psychometric temperature difference, which represents the difference between the dry bulb temperature and the cooling limit temperature, of 6°C was set in the first experiment. If cracks were not detected on dried tiles after the first experiment was over, the psychometric temperature difference was doubled in the second one. If cracks were detected in the second experiment the psychometric temperature difference was decreased to 3°C. This procedure was repeated several times and the critical drying rate was determined. The manufacturer has recorded the sorption isotherm and has shared those results with us.

3. Results and discussion

The total drying time for the dryer load of 14.000 roofing tiles as well as the max drying rate and the corresponding drying regime, which were registered in the factory before all optimization processes were activated, were respectively 76 h and 215(g/h)/m^2. One of the reasons for this large drying time

was the fact that all dryer energy requirements were obtained from the factory kilns waste heat. In other words the firing and drying cycles as well as drying and firing capacities were not coordinated well. The capacity of all chamber dryers in this drying regime was around of the capacity of one kiln. When the characterization of drying chambers and drying behavior has started the second factory kiln was in the last phase of the reconstruction process.

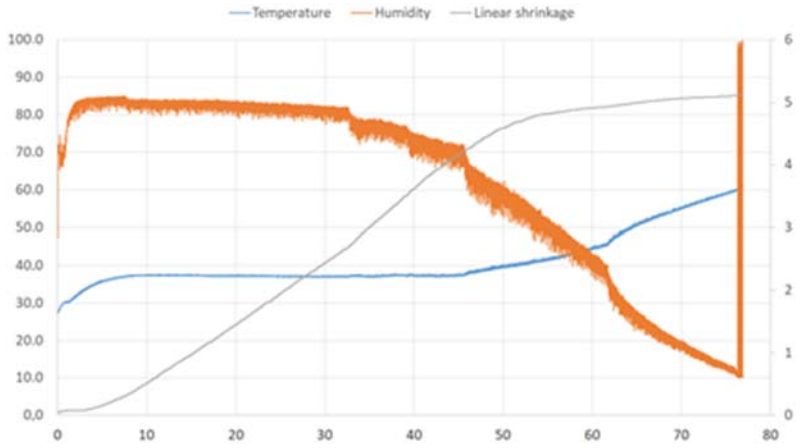

Figure 1. Drying regime registered before optimization.

The procedure for setting up the theoretically optimal drying regime which is based on ability to control the mass transport during the drying process for this clay was reported in reference [11]. It is important to state that the limiting time frame for four approximately isothermal drying segments was not specified by experience or by trial-and-error method. It was registered from Deff – MR curves which were calculated for different isothermal experimental sets. Duration of the fifth segment was limited to 90 minutes. The recommended drying regime and drying parameters were taken from reference [11] and are summarized in table 1. Dimensions of the industrial roofing tiles were 2.7 times larger than laboratory prepared samples. After the homogeneity factor and scale up factor of 2.7 were introduced duration of the recommended theoretical regime was 3 times larger than the laboratory one.

Table 1. Recommended drying parameters (Model I).

Optimal regime	Segment									
	I		II		III		IV		V	
Parameters	80%	45°C	70%	45°C	60%	45°C	60%	50°C	38%	72°C
Lab. samples (min)	257		91		44		87		90	
Ind. samples (min)	771		273		132		261		270	

It can be seen that the duration of the starting (non-optimized) drying regime is approximately 2.6 times larger than the suggested optimal one. After suggested drying air parameters were compared with the one used in the dryer it was concluded that the proposed temperature was higher than the one used in the dryer. This was the addition confirmation that further steps should be applied. Drying rate curves experimentally registered during the process of critical drying rate determination on the laboratory samples are presented at figure 2. Calculated critical drying rate was approximately two times larger than the maximal drying rate detected in the non-optimized situation. The corresponding total drying time (TDT) for lab samples under ideal conditions (at the critical drying rate) was 26 h. It is interesting that this value is similar to the proposed first model TDT (see table 1). These data has also suggested us that the optimization is justified. After the dryer inspection was finished and its

geometry, air mass flows, temperature, and humidity profiles as well as initial water content in the drying material, initial temperature of the products and the load of the dryer were collected, it was verified that before other actions are taken the first measure should be to replace all rotor mixers.

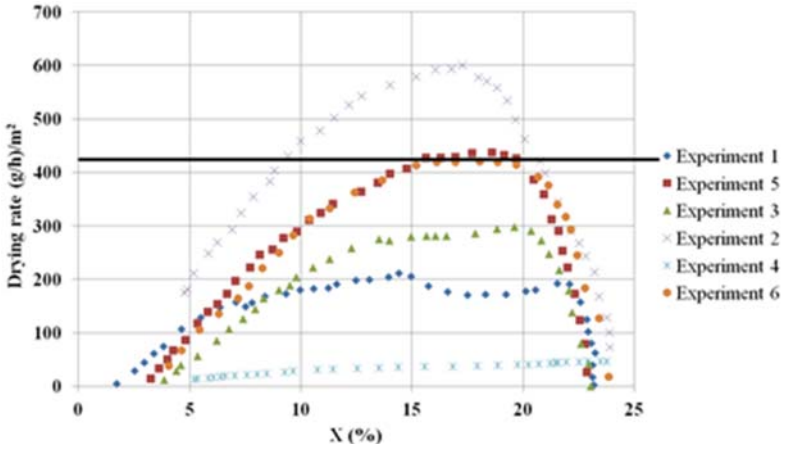

Figure 2. Critical drying rate.

Due to the fact that the reconstruction of the second kiln was not over in the planed timeline even though new rotor mixers were installed in all drying chambers the second measure was to continue the production using the same values of the drying air parameters as before the replacement. The registered drying regime is presented at figure 3.

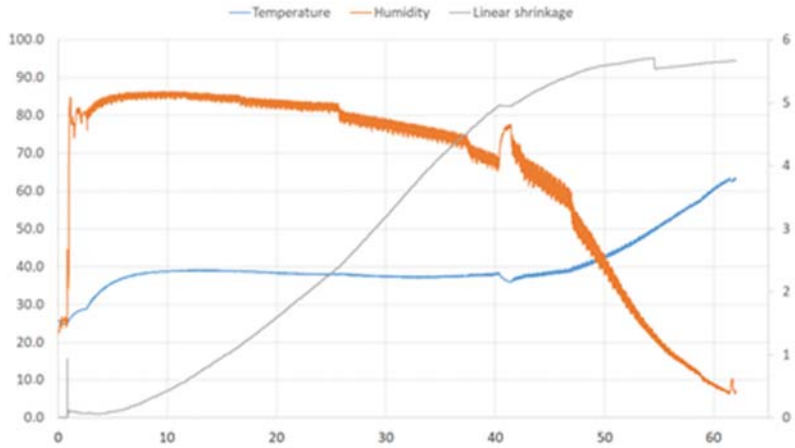

Figure 3. Drying regime after replacements of rotor mixers.

From figure 3 it can be seen that TDT was lower for 14 h. In other words TDT was reduced for approximately 19%. This was the confirmation that the first applied measure was justified. The third measure was to apply the second drying model. The simulation results are given at figure 4. It can be seen that under the ideal conditions roofing tiles could be dried for 28 h. Measured flows of hot air and cool air supply as well as measured heat transfer inside the chamber and recommended values for drying air parameters taken from model I were used in simulation model II software. Simulated TDT was 35h. Based on the simulated curves a new set points for the valve positions of supply air as well as new set points for the temperature of the feed air to the drying chamber were set. During this

process special care was taken not to exceed the simulated critical drying rate and not to exceed the maximal working temperatures of new rotor mixers.

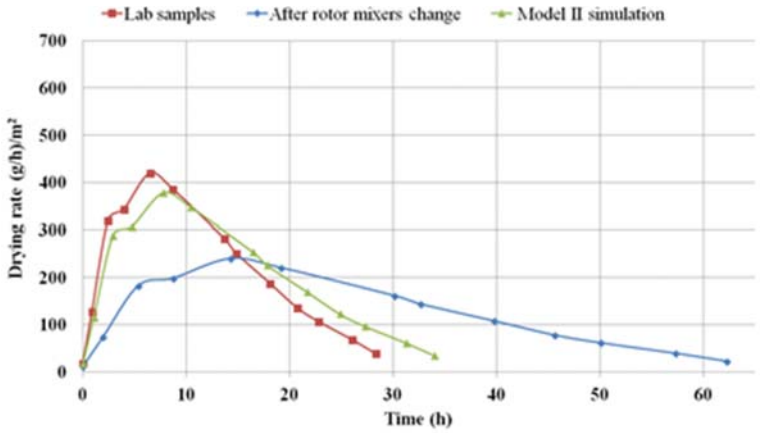

Figure 4. Experimentally registered and Model II simulated drying curve.

Simulated results has confirmed that if both kilns are working and if it is possible to produce 43% more of the green roofing tiles all chamber dryers and both kilns can operate at its maximal capacity. After the reconstruction of the second kiln was over and all recommendations were applied the TDT was reduced for 48% and the production was razed for 35%. Produced roofing tiles have satisfied all quality requirements stated in the EN 1304 standard.

4. Conclusions

The general method for industrial chamber dryer optimization was presented. The first step was to record the actual drying regime and to collect all dryer and kiln available documentation. Next step is to apply the procedure for setting up the optimal drying air parameters. This step represents a combination of isothermal experiments and simulations of corresponding Deff – MR curves. These data were then used to predict the optimal drying air parameters. The following step is to experimentally register the critical drying rate in the special recirculation laboratory dryer. All data collected up to now provides us information if the product or the dryer is the bottleneck for the optimization. If the optimization is justified geometry of the dryer, air mass flows, temperature, and humidity profiles inside the dryer as well as initial water content in the drying material, initial temperature of the products and the load of the dryer are collected. Finally the second drying model is applied and new set points for the valve positions of supply air as well as new set points for the temperature of the feed air to the drying chamber are calculated. It was shown that when all recommendations were applied in our example TDT was reduced for 48% and the production was razed for 35%.

5. References

[1] Shokouhmand H, Abdollahi V, Hosseini S, Vahidkahah K 2011 Performance optimization of a brick dryer using porous simulation approach, *Drying Technology* **29**(3) 360-370.
[2] Araujo V. M, Pereira S.A, Oliveira L.J, Bradano A.A.V, Filho B.A.F, Silva M.R, Lima B.G.A, 2019 Industrial ceramic brick drying in oven by CFD, *Materials* **12**(10) 1612 doi:10.3390/ma12101612.
[3] Dolanc. G, Vladimir. J 1997 Improvement of the drying process control in a clay product plant *IAF Proceeding* **30**(6) pp. 1575-1580.
[4] Mancuhan E. 2009, Analysis and optimization of drying of green brick in a tunnel dryer, *Drying Technology* **27**(5) 707-713.

[5] Telljohann U, Junge K, 2008 Moisture diffusion coefficients for modeling the first and second drying section of green bricks *Drying Technology* **26**(7) 855-863.
[6] Junge K, Tretau A 2007 Increasing the efficiency of drying plants through the use of modern low-energy dryers *Ziegel Ind. International* **9** pp 22-31.
[7] Karsten J, Specht E, Telljohann U, Deppe D, 2005 Drying of green bricks – Capillarity and pore volume as essential criteria for the transport processes of water and dissolved salts, *Ziegel Industrie* **8** pp 39-51.
[8] Velthuis M.F.J, Denissen M.A.J, 1997 Optimization of industrial ceramic dryers *Key Engineering Materials* ISSN 1662-9795, 132-136 **7** pp 2123-2126.
[9] Velthuis M.F.J, Denissen M.A.J, 1997 Simulation model for industrial dryers: reduction of drying times of ceramics &saving energy *Drying Technology* **15**(6-8) 1941-1948.
[10] Vasić M, Grbavčić Ž and Radojević Z 2014 Analysis of Moisture Transfer During the Drying of Clay Tiles with Particular Reference to an Estimation of the Time-Dependent Effective Diffusivity *Drying Technology* **32**(7) 829-840
[11] Vasić M, Rekecki R, Radojević Z 2018 A procedure for setting up the drying regime that is consistent with the nature and properties of clay raw material *Drying Technology* **36**(3) 267-282.
[12] Vasić M, Radojević Z 2018 Comparison and evaluation of recently reported methods for optimization of industrial drying regimes, *IOP Conf. Series: Materials Science and Engineering* **400** doi:10.1088/1757-899X/400/6/062030
[13] Rekecki R and Ranogajec J 2008 Design of ceramic miscrostructures based on waste materials *Proc. and Appl. of Ceramic* **2** 89-95

Acknowledgement

This paper was financed by ministry of education science and technological development of Serbia, contract number 451-03-68/2020-14/200012. Authors M. Vasic and Z. Radojevic are fully employed in the Institute for testing of Materials